Fabrication of high strength PVA/SWCNT composite fibers by gel spinning

Xuezhu Xu, Ahmed Jalal Uddin, Kenta Aoki, Yasuo Gotoh[1,*],

Takeshi Saito[2,3], Motoo Yumura[2]

[1] Faculty of Textile Science and Technology, Shinshu University, 3-15-1 Tokida, Ueda, Nagano 386-8567, Japan

[2] Nanotube Research Center, National Institute of Advanced Industrial Science and Technology (AIST), 1-1-1 Higashi, Tsukuba, Ibaraki 305-8565, Japan

[3] PRESTO, Japan Science and Technology Agency, 4-1-8 Honcho, Kawaguchi, Saitama 332-0012, Japan

* Corresponding author. Tel.: +81 0268 21 5366.
E-mail Address: ygotohy@shinshu-u.ac.jp (Y. Gotoh)

Abstract

High-strength composite fibers were prepared from polyvinyl alcohol (PVA) (Degree of polymerization: 1500) reinforced by single-walled carbon nanotubes (SWCNTs) containing few defects. The SWCNTs were dispersed in a 10 wt.% PVA/dimethylsulfoxide solution using a mechanical homogenizer that reduced the size of SWCNT aggregations to smaller bundles. The macroscopically homogeneous dispersion was extruded into cold methanol to form fibers by gel spinning followed by a hot-drawing. The tensile strength of the well-oriented composite fibers with 0.3 wt.% SWCNTs was 2.2 GPa which is extremely high value among PVA composite fibers ever reported using a commercial grade PVA. The strength of neat PVA fibers prepared by the same procedure was 1.7 GPa. Structural analysis showed that the PVA component in the composite fibers possessed almost the same structure as that of neat PVA fibers. Hence a small amount of SWCNTs straightforward enhanced by 0.5 GPa the tensile strength of PVA fibers. The results of mechanical properties and Raman spectra for the SWCNT composites suggest the relatively good interfacial adhesion of the nanotubes and PVA that improves the load transfer from the polymer matrix to the reinforcing phase.

1. Introduction

Single-walled carbon nanotubes (SWCNTs) [1, 2] are one of the most promising candidates as reinforcing materials. Among reinforced composite materials, composite fibers are popular approaches for utilizing SWCNTs, because SWCNTs can exert their extreme performance along the tube axis, which is coincident with the molecular chain axis in fiber. Thus, the uniaxial orientation of SWCNTs in the fiber is highly desirable.

Numerous composites fibers reinforced by SWCNTs, such as poly(*p*-phenylene benzobisoxazole) [3], polyacrylonitrile [4, 5], polyethylene [6], polypropylene [7] and polyvinyl alcohol (PVA) [8, 9] have been reported for improvement of the mechanical properties. While the introduction of SWCNTs enhances the tensile strength of the matrix fiber, exfoliation and orientation of SWCNTs in polymer matrices remain a challenge for achieving high tensile strength in SWCNT-reinforced fibers. The difficulty of exfoliation of SWCNT bundles originates from SWCNT agglomeration arising from intensive inner tube attraction due to great accumulation of van der Waals forces. The result is insolubility and inferior dispersion of SWCNTs in most organic and aqueous solvents, and the agglomerates lower the effectiveness of reinforcement by nanotubes. Although SWCNTs can be dispersed using surfactants [9, 10], there is a risk for the surfactant to remain in the polymer matrix that may detrimentally effect the final

properties of composites. Dispersion of SWCNTs by sonication is possible [11-13], but it requires long treatment time and is also reported to be destructive for SWCNTs, decreasing its strength [14]. Thus a damage-free dispersion of SWCNTs without sonication is desirable.

Some types of amphiphilic polymers, such as DNA and block copolymers containing 2-methacryloyloxyethyl phosphorylcholine can efficiently disperse SWCNTs in solution media [15, 16]. PVA also possesses amphiphilic properties as well as the ability to form fibers, and is one of the promising candidates for composite fibers with excellent mechanical properties. PVA has been utilized as a high performance fiber, and especially as a reinforcement fiber for concrete materials due to its high strength, high modulus, good adhesive strength to concrete and high alkali resistance, which enhances strength and crack resistance of concrete. With the recent development of architectural technology and requirements for earthquake resistance of buildings, increase in PVA demand as a replacement for steel fibers in concrete has been expected. Further exploration is needed to attain still higher performance for PVA fibers.

In this work, we present preparation of PVA/SWCNT composite fibers through gel spinning to enhance the tensile strength of PVA fiber by introduction of a small amount of SWCNTs with relatively low defect. We also demonstrate a favorable method of

dispersion that yields nanoscale dispersions of SWCNT bundles in PVA solution without addition of surfactant or use of sonication, to preclude nanotube destruction.

2. Experimental

2.1 *Materials*

PVA chip (Poval-HC, Kuraray Co. Ltd.) with degree of polymerization (DP) and saponification ca. 1500 and 99.9%, respectively, was used in this work. The SWCNTs were synthesized by a method called 'enhanced-Direct Injection Pyrolytic Synthesis' (e-DIPS) by a co-research group of the National Institute of Advanced Industrial Science and Technology (AIST). SWCNTs had a purity of 97.5%, average tube diameter ca. 2 nm, and average tube length 10-20 μm. SWCNTs were used without purification or treatment. Dimethyl sulfoxide (DMSO) purchased from Wako Chemicals Industry Ltd. was used as received.

2.2 *Sample Preparation*

PVA chip was washed with distilled water to remove impurities such as sodium acetate, and the polymer was dissolved in DMSO at 100 °C with agitation. Two PVA/DMSO solutions were prepared, with PVA concentration 10 and 20 wt.%. SWCNTs were added to the 10 wt.% PVA solution at three SWCNT contents, namely 0.05, 0.1 and 0.3 wt.%

relative to PVA content. The mixtures were then homogenized with a homogenizer (PH91, SMT Co. Ltd. Japan) at rotational speed 18,000 rpm at 95 ℃ for 10 min. Sufficient 20 wt.% PVA/DMSO solution was gradually added to adjust the PVA concentration to 15 wt.% in the final solution. The mixture was stirred with mild rotation at 100 ℃ for 2 h, and then deaerated in an oven at 80 ℃ for 12 h prior to spinning. In this way, 15 wt.% PVA/DMSO solutions with varying concentrations of SWCNTs were prepared as spinning dope.

2.3 *Gel Spinning and hot drawing*

Gel spinning was carried out using a syringe pump and a syringe with needle. The temperature of a heater surrounding the syringe was set at 120°C, and the PVA/SWCNT/DMSO dispersion was injected at 0.38 ml min^{-1} through a 0.57 mm diameter hole needle into cold methanol maintained at a temperature between -10 and -15 °C. The as-spun gel fibers were kept rotating in methanol at room temperature for more than 24 h and subsequently dried in a vacuum oven at 60 ℃ for 4 h. The fibers were drawn at 220 °C in an oven using a manual stretching apparatus. Draw ratios of samples are mentioned in the 'Result and Discussion' section (Table 1).

2.4 *Measurements*

Scanning electron microscopy (SEM) was conducted with a Hitachi S-2380N

instrument after sputter coating the samples with platinum.

Transmission electron microscopy (TEM) images were obtained with a JEOL JEM-2010 using a carbon-sputtered sample.

Raman spectra were recorded with a Hololab 5000 instrument using a 532 nm laser with 50 mW power. The power of the irradiated laser was adjusted by an attenuator not to change the sample structure by laser irradiation. The measurement was carried out by 50 scans of accumulation for exposure time of 5 sec for each scan. For evaluation of SWCNTs orientation in the composite fiber, Raman scattering intensity of SWCNTs was measured in the VV measurement configuration (I^{VV}_{fiber}). In VV configuration, the polarizer and analyzer were parallel to each other.

Ultraviolet-visible (UV-Vis) spectroscopy was carried out using a Hitachi U-3500 UV-Vis spectrophotometer. Measurements were made at scanning speed of 300 nm min^{-1} in the wavelength range of 185-800 nm by the transmission method.

Wide-angle X-ray diffraction (WAXD) was carried out with a Rigaku Rotorflex RU200B X-ray generator operated at 40 kV and 150 mA. The radiation was Ni-filtered Cu-K_α (wavelength 0.1542 nm).

Tensile testing was performed with an A&D Tensilon RTC-1250A at room temperature with a 50 N load cell, gauge length 20 mm and crosshead speed 20 mm min^{-1}. The

experimental results were evaluated as the averages of at least 10 measurements.

3. Results and Discussion

To clarify the quality of SWCNTs of this study, Raman spectroscopic measurement was conducted. Figure 1 shows Raman spectrum of pristine SWCNTs. The bands were observed at 1341 cm^{-1} (D band) and 1592 cm^{-1} (G band), corresponding to amorphous carbon impurities and carbon nanotubes, respectively [17]. The band intensity at 1341 cm^{-1} was extremely low, while the G-band had much higher intensity. The intensity ratio (I_G/I_D) is usually utilized for characterization of the structural perfection of carbon-based materials. In the present case the I_G/I_D value was 133, implying that the SWCNTs used had high degree of perfection. The extremely low intensity of the D band is attributed to the relatively low defect of nanotubes in the raw material. Even a small amount of structural defects greatly reduces the strength of ultra-high strength materials. This Raman result suggested the possibility that such high structural perfection of SWCNTs could lead to high strength composite fibers. As shown in the inset of Figure 1, the radial breathing mode (RBM) band was observed at 137 cm^{-1} and the diameter of the tube from the RBM band was estimated as 1.8 nm from the experimental relationship of $d = 248/\nu$ (d: diameter of CNT (nm), ν:Raman shift (cm^{-1})) [18].

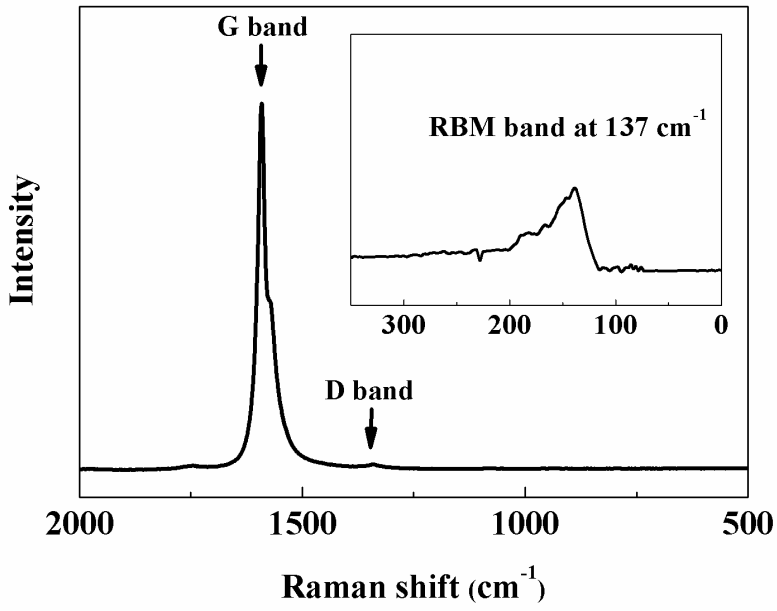

Figure 1 Raman spectrum of pristine SWCNTs.

As shown in Figure 2, TEM measurement was carried out to observe the pristine SWCNTs. Each single tube had diameter ca. 2 nm, which was approximately same with the result of Raman measurement, and the diameter of bundles 10-20 nm was observed. The observed darker spherical particles are the metal iron catalyst for SWCNT synthesis.

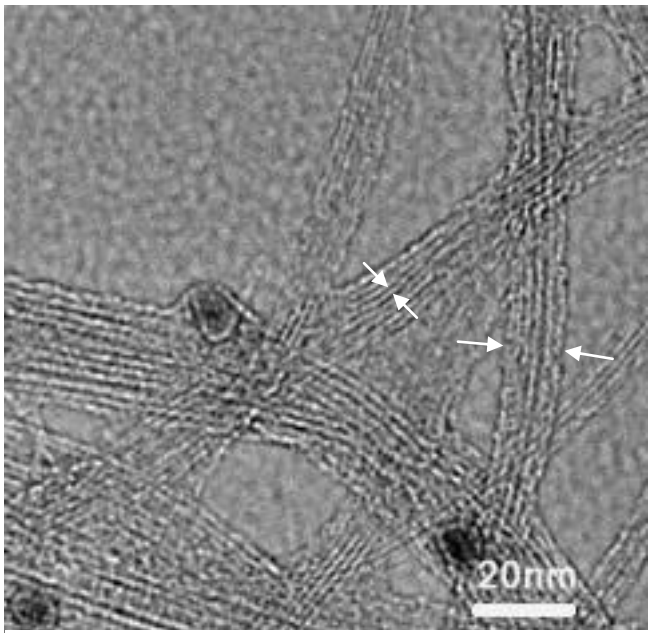

Figure 2 TEM image of pristine SWCNTs.

For gel spinning of PVA, DMSO and methanol were selected as solvent and coagulant, respectively, because these are frequently used industrially for producing high strength PVA fibers [19-21]. SWCNT dispersions in neat DMSO and PVA/DMSO solution were prepared using a mechanical homogenizer as described in the 'Experimental' section.

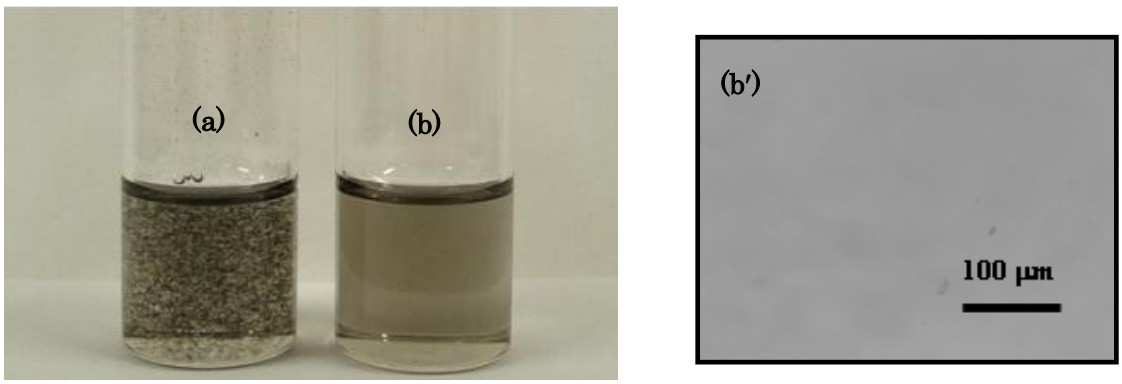

Figure 3 (a) DMSO/SWCNT (0.3 wt.%) dispersion, (b) PVA/DMSO/SWCNT (0.3

wt.%), and (b′) optical micrograph of (b). In both (b) and (b′) the PVA concentration is 10 wt.%.

Figure 3 shows photographs and an optical microscope image of dispersions containing 0.3 wt.% SWCNTs with and without 10 wt.% PVA. Each was prepared by homogenization for 10 min. In the DMSO system, the visible aggregates indicate poor dispersion of SWCNTs. In contrast, SWCNTs were dispersed homogeneously at the macroscopic level in the presence of PVA. This dispersion was unchanged in appearance and stable for at least one month. The Raman spectrum of SWCNTs and the degree of polymerization of PVA were unchanged after homogenization, which means that defects in SWCNTs and chain dissociation of PVA were not generated at the microscopic scale. It was reported that defects introduced by oxidative pitting during composite preparation markedly reduce fracture strength, and extensive pitting leads to lower modulus [22, 23]. Moreover, the other potential source of large defects of nanotubes was found by the use of sonication that caused strength underperformance [11]. In the present study, the direct physical homogenizing process in the presence of PVA made SWCNT dispersion in DMSO possible without sonication, and this procedure is preferable for dispersing SWCNTs. In addition, the pristine SWCNTs are cottony mat sample and likely to show weaker interaction between the tubes, making it

possible to easily disperse in PVA/DMSO solution solely by mechanical homogenization. In one experiment, pristine SWCNTs were wetted with DMSO and dried by vaporization of the DMSO, and the SWCNTs then became difficult to disperse homogeneously in PVA/DMSO solution by our homogenizing process. The actual reason is difficult to clarify. It is thought that the cohesive force between tubes was enhanced by capillary force during the drying of DMSO. Hence the initial surface state of SWCNTs seems to have influence on its dispersion.

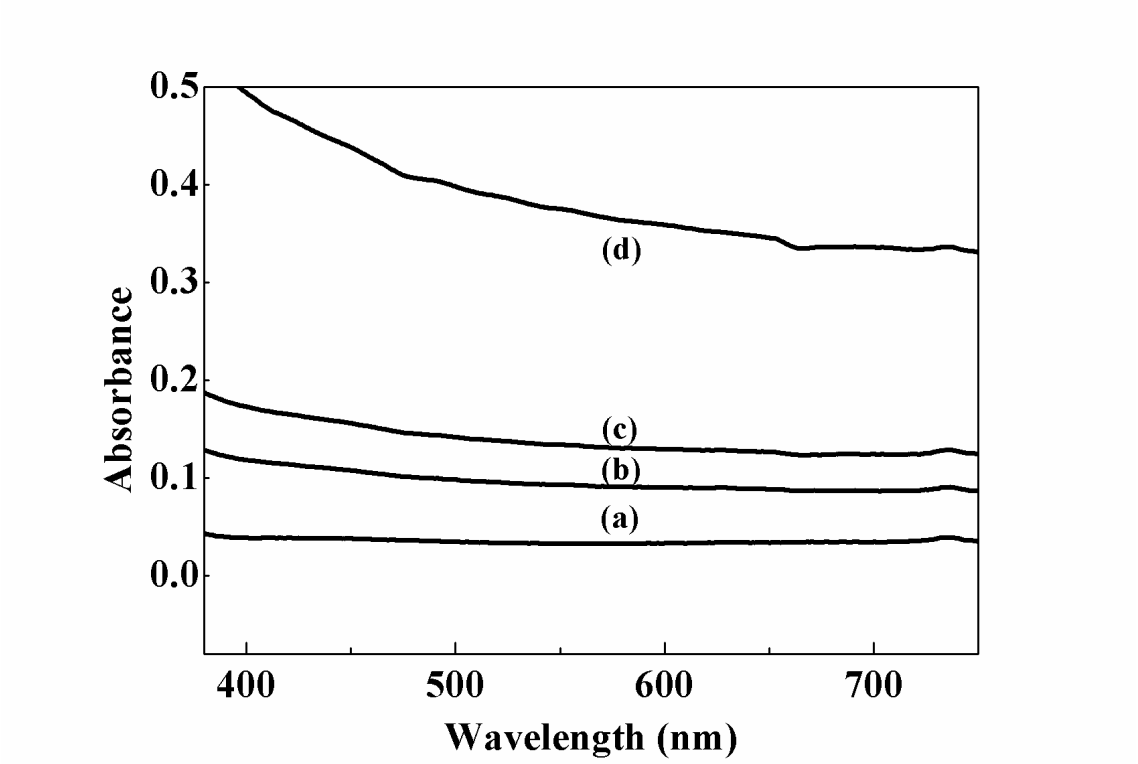

Figure 4 UV-Vis spectra of PVA/SWCNT dispersions with different SWCNT contents. (a) PVA solution, (b) PVA/SWCNT (0.05 wt.%) solution, (c) PVA/SWCNT (0.1 wt.%) solution, (d) PVA/SWCNT (0.3 wt.%) solution. PVA concentration in DMSO was 10

wt.% in all the samples.

Further exploration of the dispersion quality of SWCNTs in PVA/DMSO solution was carried out by UV-Vis spectrophotometry (Figure 4). When SWCNTs are exfoliated, many separated sharp peaks are generally observed in the UV-Vis spectrum due to van Hove transitions that arise from electronic transitions within one-dimensional density of states [5]. Conversely, three-dimensional materials have continuous densities of state, and consequently separated optical absorptions by van Hove transitions are not clearly found in SWCNT bundles. In our experiment, there was no discernible absorption peak in the wavelength range as showed in Figure 4, suggesting that bundles of SWCNTs were not completely exfoliated in PVA/DMSO solution by the mechanical homogenization process.

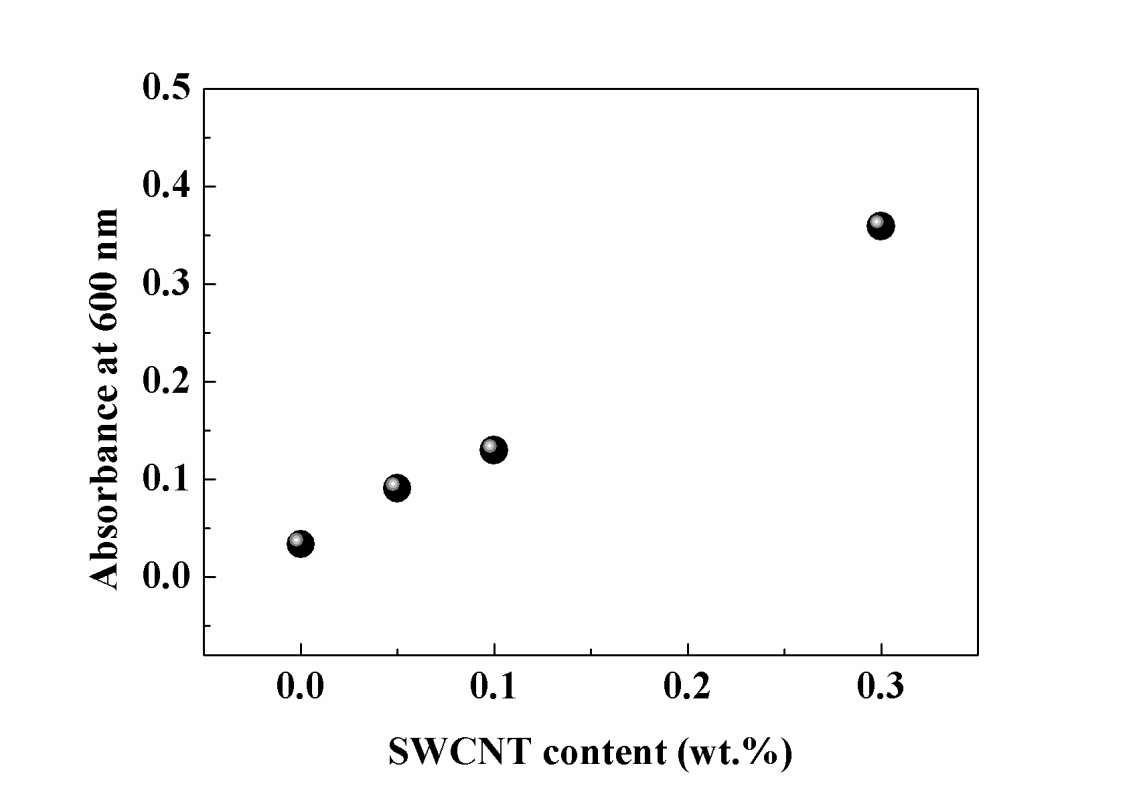

Figure 5 Absorbance at 600 nm in UV-Vis spectra of PVA/SWCNT dispersions with varying SWCNT content.

Figure 5 shows the relationship between SWCNT content and absorbance at 600 nm in UV-Vis spectra of PVA/SWCNT dispersions. The absorbance increased linearly with SWCNT content, indicating that the dispersion states of SWCNTs were almost the same in all dispersions.

The dispersion state of SWCNTs in PVA matrix was directly observed by TEM. Figure 6 shows a TEM image of PVA/SWCNT (0.1 wt.%) thin film prepared by spin-casting PVA/DMSO/SWCNT spinning solution. The bundle size of SWCNTs

could be observed less than 10 nm, thus smaller than that of pristine SWCNTs shown in Figure 1. The mechanical homogenization in PVA solution reduced the bundle size of SWCNTs and made homogeneous and stable dispersions at the microscopic level.

Although the SWCNTs in the PVA matrix remained in bundle form, the bundle sizes became smaller that was attributed mainly to both better dispersibility of pristine SWCNTs and good affinity of PVA with SWCNTs. The addition of PVA obviously improved the dispersion and the stability of SWCNTs in the dispersion. This effect was due to the interaction between the SWCNTs surface and PVA, which made it possible for PVA molecules to wrap SWCNTs, thus preventing their re-aggregation. To confirm the interaction of SWCNTs and PVA, a PVA/SWCNT/DMSO solution (same with the sample of Figure 3 b) was diluted with distilled water, then the coagutation containing SWCNTs was generated, and the coagulation was collected by centrifugation and repeatedly washed with distilled water. After washing, the SWCNTs were observed by TEM (Figure 7). The coagulant was well washed with water, a good solvent of PVA, however, PVA still covered the SWCNT surface indicating the good existence of adhesive force between SWCNTs and PVA.

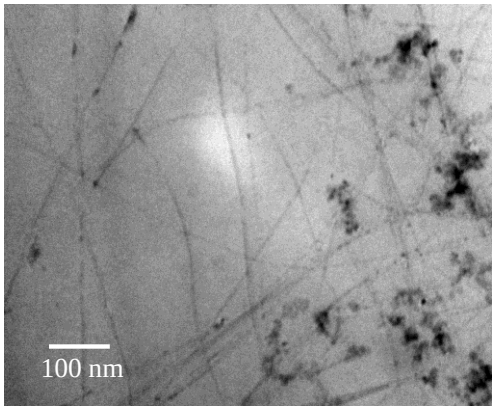

Figure 6 TEM image of PVA/SWCNT (0.3 wt.%) spin-casted film.

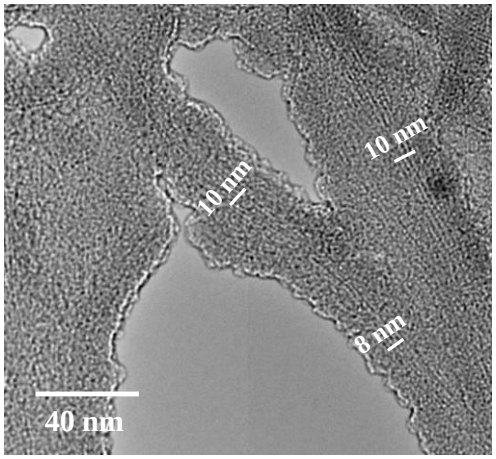

Figure 7 TEM image of PVA/SWCNT aggregate after washing with distilled water.

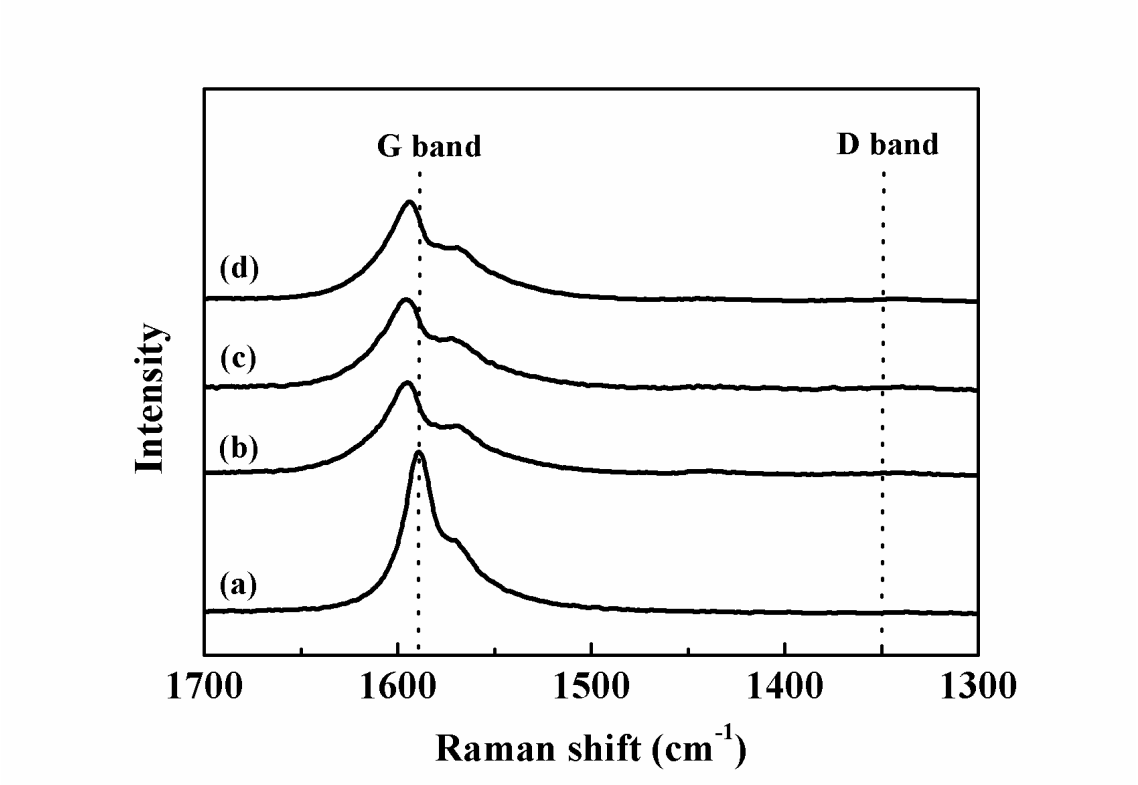

Figure 8 Raman spectra of (a) pristine SWCNT, (b) PVA/SWCNT (0.05 wt.%), (c) PVA/SWCNT (0.1 wt.%), (d) PVA/SWCNT (0.3 wt.%) fibers.

Raman spectroscopy was utilized to obtain information on the influence of PVA on the electronic structure of the SWCNTs. Figure 8 shows Raman spectra of neat SWCNTs and PVA/SWCNT undrawn composite fibers with SWCNT concentrations 0.05, 0.1 and 0.3 wt.%. The peaks of the G bands for the composites were shifted to a higher wave number by ca. 7 cm^{-1}. Previous experimental work has shown that doping SWCNTs with either electron donors or acceptors results in an obvious shift of certain characteristic Raman vibration modes. The upshift of the Raman band at about 1590

cm^{-1} was attributed to charge transfer between SWCNTs and matrix polymer [24], implying interaction between them. Thus, this result was a qualitative evidence to show the affinity of SWCNTs to PVA matrix.

Concering spinning, the viscosity of the spinning solutions doped with SWCNTs was increased (neat PVA:1.05 Pa·s, PVA/SWCNT (0.3 wt.%):1.56 Pa·s at 120 °C), consequently higher pressure was necessary to extrude the composite dispersions. Moreover, those dispersions became more difficult to collapse during spinning, and the length of the thread line of the solution passed though the air gap between the needle tip to coagulant was increased with increase of loaded SWCNTs (neat PVA: 0 mm, and PVA/SWCNT (0.3 wt.%): 11 mm). This result indicated that the spinnability was enhanced by incorporating SWCNTs.

The gel-spun neat PVA fibers exhibited good drawability in the hot-drawing process and a maximum draw ratio of 26 was achieved. By introduction of SWCNTs the maximum draw ratio of the composite fibers was reduced slightly to 23-24. However, the appearance of the drawn fibers was smooth and homogeneous, and almost the same as neat PVA fiber, as shown in the SEM images of Figure 9.

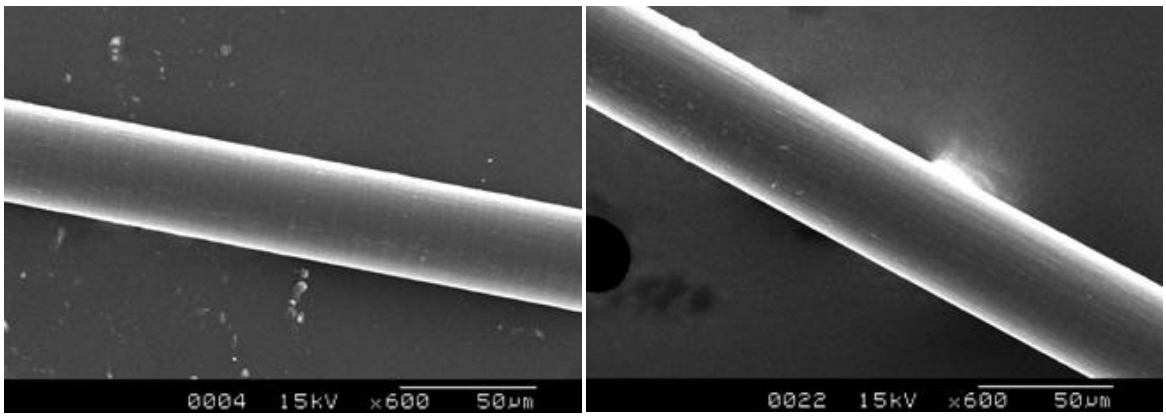

Figure 9 SEM images of (a) neat PVA and (b) PVA/SWCNT (0.3 wt%) drawn fibers.

Table 1 Properties of drawn fibers of neat PVA and PVA/SWCNT composites

Sample	Draw ratio	Diameter (μm)	Tensile strength (GPa)	Young's modulus (GPa)	Elongation (%)
Neat PVA	26	38±3	1.7±0.1	28±3	11±0.8
PVA/SWCNT (0.05 wt.%)	24	42±2	2.1±0.1	30±3	11±0.1
PVA/SWCNT (0.1 wt.%)	24	40±4	1.9±0.1	33±3	10±0.9
PVA/SWCNT (0.3 wt.%)	23	42±4	2.2±0.1	36±4	10±0.6

The tensile properties of neat PVA and PVA/SWCNT composite drawn fibers are given in Table 1, and Figure 10 shows typical stress-strain curves for drawn fibers of neat PVA and the PVA/SWCNT (0.3 wt.%) composite. The shapes of the stress-strain curve for the composite fiber are almost linear and similar to that of neat PVA. However,

the slope and the end point are higher for the composite sample. The data in Table 1 show that the tensile strength and Young's modulus of the PVA/SWCNT composite fibers are significantly improved compared to the neat PVA fibers. Notably, a tensile strength of 2.2 GPa was achieved by incorporation of 0.3 wt.% SWCNT loading, thus a small proportion of SWCNTs significantly enhanced the tensile properties of PVA fibers.

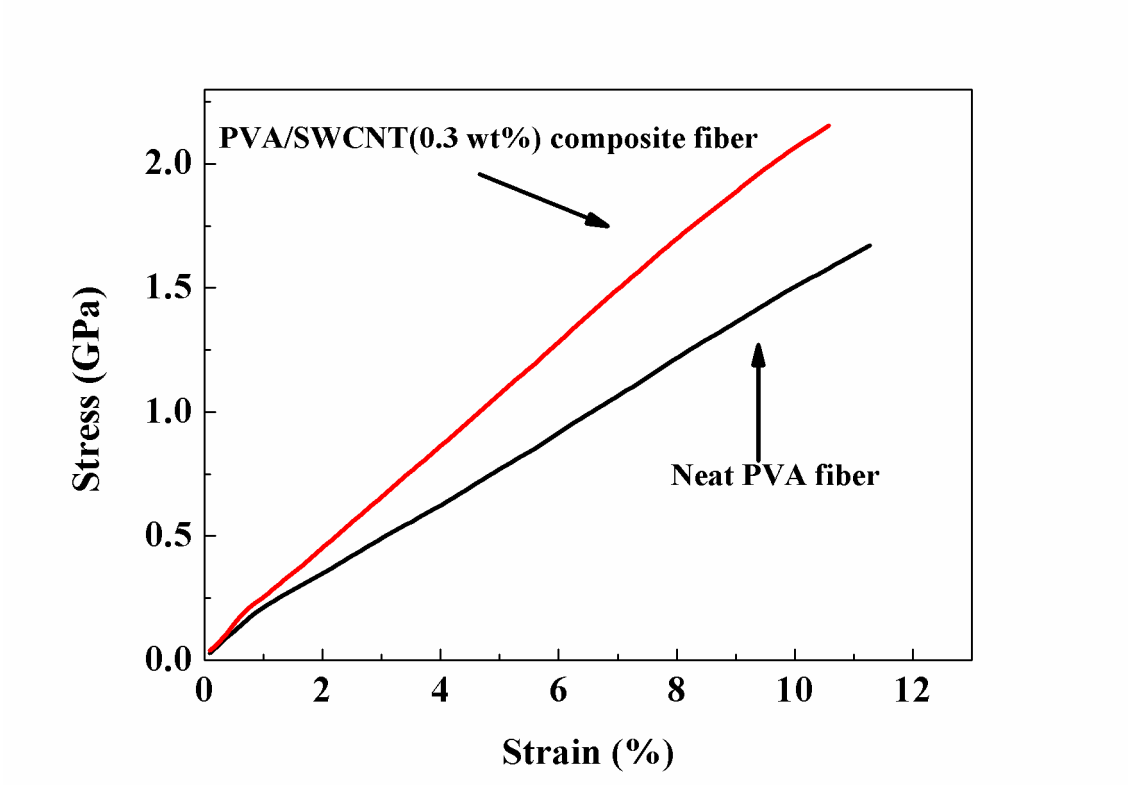

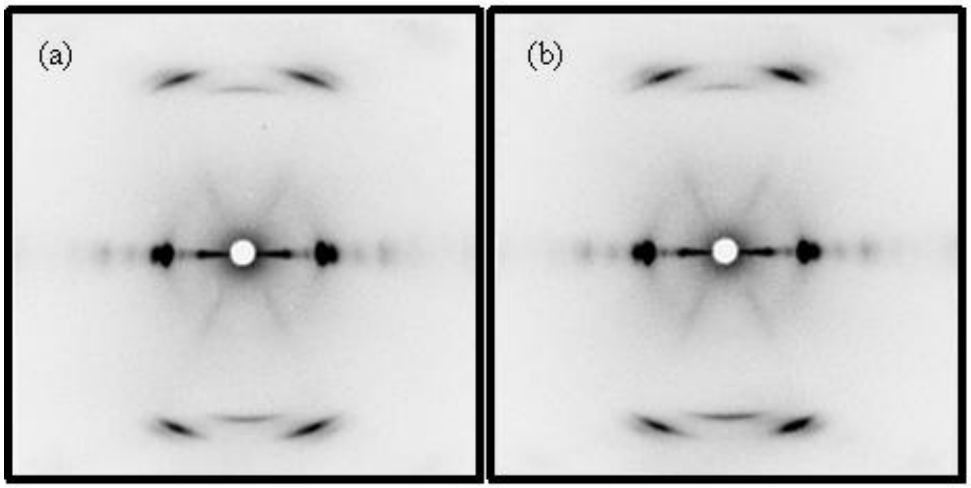

Figure 11 WAXD photographs of (a) neat PVA and (b) PVA/SWCNT (0.3 wt.%) drawn fibers.

To understand the reason for the enhancement of tensile properties, structural analysis was carried out using X-ray diffraction. Figure 11 shows WAXD photgraphs of drawn fibers of neat PVA and PVA/SWCNT (0.3 wt.%) composite. The two patterns are almost identical. The degrees of crystallite orientation for the PVA component were determined from the diffraction peak of (101) plane as 0.984 and 0.990 for neat PVA and the composite, respectively. For each sample, the crystallite size determined from (101) using Scherrer's equation are coincident at 5 nm. Thus, the PVA component makes virtually equal contributions to the tensile strength of both fibers, and the tensile strength enhancement is attributable to the extremely high strength of SWCNTs.

Since the real tensile strength of SWCNTs was not known, the strength was roughly estimated from the equation [25];

$$\sigma_c = \eta_L \eta_o V_f \sigma_f + (1 - V_f)\sigma_m$$

where σ_c, σ_f, and σ_m are the strength of composite, reinforcing fiber and matrix polymer, respectively. V_f is the volume fraction of loaded reinforcing fiber. The fiber length efficiency factor η_L varies between 0 and 1. The orientation factor η_o is equal to 1 for fully aligned fibers. This equation is used to evaluate the nanotube contributions to the strength of uniaxial composites if the strengths of the matrix, the composite and the nanotube are known. In this case, we experimentally determined η_o to know SWCNTs orientation using the polarized Raman intensity. Figure 12 shows the G-band intensity as a function of fiber rotation angle (φ) for PVA/SWCNT (0.3 wt.%) drawn fibers. The intensity is decreased as the angle, φ between the polarization direction and fiber axis increases from 0 to 90 °. From the following equation [26] for SWCNT orientation distribution function, the orientation order parameters for SWCNTs in the composite are determined;

$$I^{VV}_{Fiber}(\Phi) \propto \left(\cos^4 \Phi - \frac{6}{7}\cos^2 \Phi + \frac{3}{35} \right) \langle P_4(\cos\theta) \rangle + \left(\frac{6}{7}\cos^2 \Phi - \frac{2}{7} \right) \langle P_2(\cos\theta) \rangle + \frac{1}{5}$$

, where the Raman intensity in the VV mode (I^{VV}_{fiber}) is proportional to second- and forth-order orientation parameters (<P_2(cosθ)> and <P_4(cosθ)>). θ is the angle between the SWCNT axis and the composite fiber axis. <P_2(cosθ)> is experimentally determined

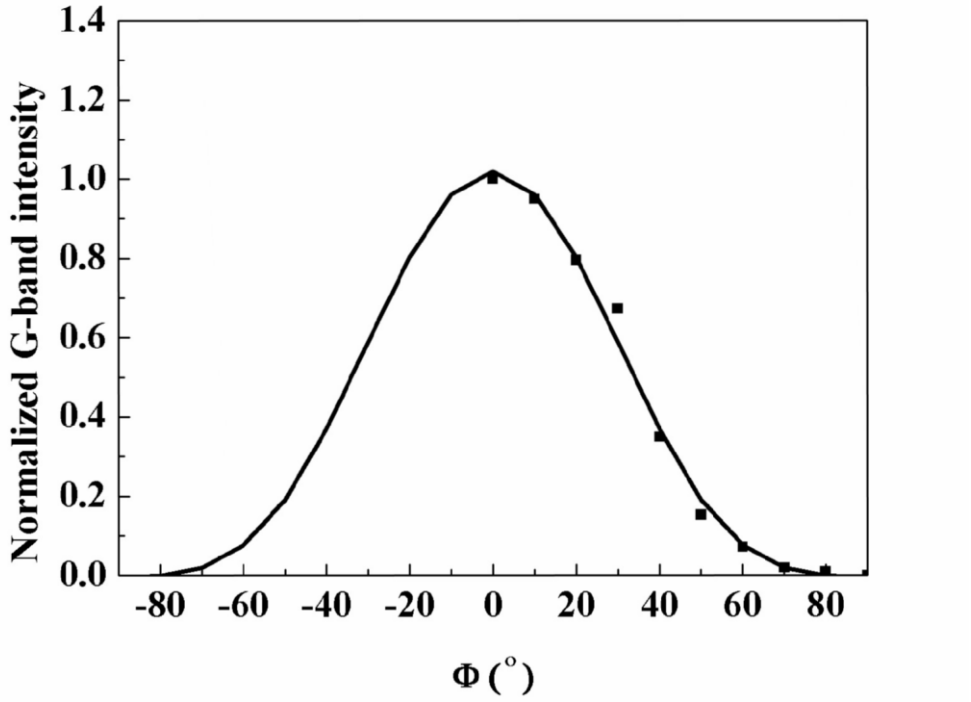

Figure 12 Normalized G-band intensity as a function of fiber rotation angle (φ) for PVA/SWCNT (0.3 wt.%) drawn fiber.

parameter (η_o).

From Figure 12, the value of η_o (f_{SWCNTs}) was determined as 0.96.

Since we do not know the real η_L value, an effective nanotube strength that incorporates only the length efficiency of the nanotubes, given by $\sigma_{eff} = \eta_L \sigma_f$, is used. According to our measurements σ_c and σ_m have the values 2.2 and 1.7 GPa, respectively, and V_f = 0.003. This analysis gives effective nanotube strength of 175 GPa, which is relatively comparable to the highest measured strength of carbon nanotubes (ca. 110 GPa) [11]. The SWCNTs used in this study have relatively high perfection of graphene structure as

shown in the Raman spectrum of Figure 1. On those grounds the estimated strength is likely to be reasonable. Of course, the reinforcing effect needs efficient interfacial stress transfer from PVA matrix to SWCNTs. As shown by the Raman spectra of the composite in Figure 8, interactions based on charge transfer might bring the considerably good interfacial adhesion.

Table 2 Tensile properties of PVA/SWCNT drawn fibers.

SWCNT content (wt.%)	Tensile Strength (GPa)	Young's modulus (GPa)	Elongation (%)	Reference
0.35	0.15	15	3	Vigolo (2000) [27]
60	1.8	80	105	Dalton (2003) [28]
3	1.1	35.8	8.8	Zhang (2004) [9]
0.35	1.6	14.5	11	Miaudet (2005) [29]
1	1.2	-	17	Wang (2007) [25]
1	2.6	71	6.2	Minus (2009) [30]
0.3	2.2	36	10	Current work

To date, many attempts have been made to develop higher strength and higher modulus PVA/SWCNT composites, because fabrication of PVA composites can utilize solution techniques to mix and disperse nanofillers, and these techniques are easily applied to traditional solution spinning technology. The mechanical properties that have been achieved for PVA/SWCNT composite fibers, as reported in the literature, are tabulated in Table 2. The highest strength of the composite was achieved at 2.6 GPa [30] while using the PVA of much higher molecular weight (DP: 18,000). But our results show remarkable SWCNT reinforcement for PVA matrix. The tensile strength of the composite in this study has exceeded most of past results, although the neat PVA fiber with conventional DP has even high strength of 1.7 GPa. The improvement of the tensile strength originated from SWCNTs with high degree of perfection of nanotubes and relatively well dispersed state. Enhancement of tensile strength can be achieved by using a commercial DP grade of PVA, loading of a small content of SWCNTs without any purification, and a simple mechanical homogenizing process for shorter time. These features are beneficial for industrial scale production of PVA/SWCNT composite fibers.

4. Conclusions

PVA/SWCNT/DMSO dispersions can be obtained using a mechanical homogenizer without surfactant or sonication. Due to their small length, SWCNTs retained a pristine structure through physical stirring even at high speed. The PVA/SWCNT/DMSO dispersions were successfully spun into smooth-surfaced composite fibers through gel spinning. PVA/SWCNT (0.3 wt.%) composite fibers notably exhibit tensile strength as high as 2.2 GPa, an increase of 500 MPa from neat PVA fiber strength with loading of only 0.3 wt.% SWCNTs. The draw ratio and resultant tensile strength achieved in this study for the gel-spun PVA/SWCNT composite fibers are the highest reported values for commercial grade PVA. However, the increase in Young's modulus and elongation at break are not significant compared with previously reported values. This could be due to deficiencies of SWCNTs loading in our work. We noticed that much higher loading of nanotubes resulted in high viscosity PVA/SWCNT/DMSO dispersions that were difficult to inject through a syringe pump during gel spinning. Thus more sophisticated methodology is needed to enable higher SWCNT loading for fabrication of higher strength PVA/SWCNT composite fibers. In addition, the processing conditions such as concentration of PVA and drawing technique can further be optimized. This work provides the basis for further investigations of those aspects of the process.

Acknowledgments

The authors acknowledge the supply of PVA pellets from Kuraray Ltd, Japan. The authors are indebted to the Ministry of Education, Culture, Sports, Science and Technology of Japan for support of this work through a Grant-in-Aid for Global COE program. This work is also partially supported by the New Energy and Industrial Technology Development Organization (NEDO). The authors gratefully thank to Takuya Tetsumoto, Faculty of Textile Science and Technology, Shinshu University, Japan for his help of TEM measurements.

References

[1] Iijima S, Helical microtubules of graphitic carbon. Nature 1991; 354 (6348): 56–8.

[2] Mikhail EI, Daniel EP, Richard J, Sandip N, Robert CH, Comparison of analytical techniques for purity evaluation of single-walled carbon nanotubes. J Am Chem Soc 2005; 127(10): 3439–48.

[3] Kumar S, Dang TD, Arnold FE, Bhattacharyya AR, Min BG, Zhang X, et al. Synthesis, structure, and properties of PBO/SWNT composites. Macromolecules 2002; 35(24): 9039–43.

[4] Sreekumar TV, Liu T, Min BG, Guo H, Kumar S, Hauge RH, et al. Polyacrylonitrile single-walled carbon nanotube composite fibers. Adv Mater 2004; 16(1): 58–61.

[5] Chae HG, Minus ML, Kumar S, Oriented and exfoliated single wall carbon nanotubes in polyacrylonitrile. Polymer 2006; 47(10): 3494–504.

[6] Ruan S, Gao P, Yu TX, Ultra-strong gel-spun UHMWPE fibers reinforced using multiwalled carbon nanotubes. Polymer 2006; 47(5): 1604-11.

[7] Kearns JC, Shambaugh RL, Polypropylene fibers reinforced with carbon nanotubes. J Appl Polym Sci 2002, 86(8): 2079–84.

[8] Zhang X, Liu T, Sreekumar TV, Kumar S, Moore VC, Hauge RH, et al. Poly(vinyl alcohol)/SWNT composite film. Nano Lett 2003; 3 (9):1285–8.

[9] Zhang X, Liu T, Sreekumar TV, Kumar S, Hu X, Smith K, Gel spinning of PVA/SWNT composite fiber. Polymer 2004; 45(26): 8801–7.

[10] Liu L, Barber AH, Nuriel S, Wagner HD, Mechanical properties of functionalized single-walled carbon-nanotube/poly(vinyl alcohol) composites. Adv Funct Mater 2005; 15(6): 975–80.

[11] Peng B, Locascio M, Zapol P, Li S, Mielke SL, Schatz GC, et al. Measurements of near-ultimate strength for multiwalled carbon nanotubes and irradiation-induced crosslinking improvements. Nature nanotechnology 2008; 3(10): 626–31.

[12] Yi W, Malkovshiy A, Chu Q, Sokolov AP, Colon ML, Meador M, et al. Wrapping of single-walled carbon nanotubes by a π-conjugated polymer: the role of polymer

conformation-controlled size selectivity. J Phys Chem B 2008; 112 (39): 12263–9.

[13] Xu Y, Pehrsson PE, Chen L, Zhang R, Zhao W, Double-stranded DNA single-walled carbon nanotube hybrids for optical hydrogen peroxide and glucose sensing. J Phys Chem C 2007; 111 (24): 8638–43.

[14] Lu KL, Lago RM, Chen YK, Green MLH, Harris PJF, et al. Mechanical damage of carbon nanotubes by ultrasound. Carbon 1996; 34(6): 814–6.

[15] Zheng M, Jagota A, Semke ED, Diner BA, Mclean RS, Lustig SR, et al. DNA-assi sted dispersion and separation of carbon nanotubes. Nature Materials 2003; 2(5): 338–42.

[16] Nakashima N, Okuzono S, Murakami H, Nakai T, Yoshikawa K. DNA dissolves single-walled carbon nanotubes in water, Chem Letters 2003, 32 (5), 456–7.

[17] Khan MMR, Gotoh Y, Morikawa H, Miura M, Fujimori Y, et al. Carbon fiber from natural biopolymer bombyx mori silk fibroin with iodine treatment. Carbon 2007; 45(5): 1035–42.

[18] Jorio A, Saito R, Hafner JH, Lieber CM, Hunter M, McClure T, et al, Structural (n,m) determination of isolated single-wall carbon nanotubes by resonant Raman scattering. Phys Rev Lett 2001, 86 (6), 1118–21.

[19] Yamaura K, Kumakura R, Gel-spinning of partially saponificated poly(vinyl alcohol). J Appl Polym Sci 2000; 77(13): 2872–6.

[20] Cha W, Hyon SH, Ikada Y, Gel spinning of polyvinyl alcohol from dimethyl sulfoxide/water mixture. J Polym Sci, Part B: Polymer Physics 1994; 32(2): 297.

[21] Tanigami T, Yano K, Yamaura K, Matsuzawa S, Anomalous swelling of polyvinyl alcohol film in mixed-solvents of dimethylsulfoxide and water. Polymer 1995; 36(15): 2941–6.

[22] Mielke SL, Troya D, Zhang S, Li JL, Xiao S, Car R, et al. The role of vacancy defects and holes in the fracture of carbon nanotubes. Chem Phys Lett 2004; 390(4-6): 413–20.

[23] Zhang S, Mielke SL, Khare R, Troya D, Ruoff RS, et al. Mechanics of defects in carbon nanotubes: atomistic and multiscale simulations. Phys Rev B 2005; 71(11): 115403–10.

[24] Wise KE, Park C, Siochi EJ, Harrison JS, Stable dispersion of single wall carbon nanotubes in polyimide: the role of noncovalent interactions. Chem Phys Lett 2004; 391(4-6): 207–11.

[25] Wang Z, Ciselli P, Peijs T, The extraordinary reinforcing efficiency of single-walled carbon nanotubes in oriented poly(vinyl alcohol) tapes. Nanotechnology

2007; 18 (45): 455709–18.

[26] Liu T, Kumar S, Quantitative characterization of SWNT orientation by polarized Raman spectroscopy. Chem Phys Lett 2003; 378 (3–4): 257–62.

[27] Vigolo B, Pénicaud A, Coulon C, Sauder C, Pailler R, journet C, et al. Macroscopic fibers and ribbons of oriented carbon nanotubes. Science 2000; 290 (5495): 1331–4.

[28] Dalton AB, Collins S, Munoz E, Razal JM, Ebron VH, et al. Super-tough carbon-nanotube fibres. Nature 2003; 423(6941): 703.

[29] Miaudet P, Badaire S, Maugey M, Derré A, Pichot V, et al. Hot-drawing of single and multiwall carbon nanotube fibers for high toughness and alignment. Nano Lett 2005; 5 (11): 2212–5.

[30] Minus ML, Chae HG, Kumar S, Interfacial crystallization in gel-spun poly(vinyl alcohol)/single-wall carbon nanotube composite fibers. Macromol Chem Phys 2009; 210 (21): 1799–1808.